Title

Reducing secondary organic aerosol formation from gasoline vehicle exhaust

Journal

Proceedings of the National Academy of Sciences of the United States of America, 114(27)

ISSN

0027-8424

Authors

Zhao, Yunliang
Saleh, Rawad
Saliba, Georges
et al.

Publication Date

2017-07-03

DOI

10.1073/pnas.1620911114

Peer reviewed

Reducing secondary organic aerosol formation from gasoline vehicle exhaust

Yunliang Zhao[a,b], Rawad Saleh[a,b,1], Georges Saliba[a,b], Albert A. Presto[a,b], Timothy D. Gordon[a,2], Greg T. Drozd[c], Allen H. Goldstein[c], Neil M. Donahue[a,d], and Allen L. Robinson[a,b,3]

[a]Center for Atmospheric Particle Studies, Carnegie Mellon University, Pittsburgh, PA 15213; [b]Department of Mechanical Engineering, Carnegie Mellon University, Pittsburgh, PA 15213; [c]Department of Environmental Science, Policy and Management, University of California, Berkeley, CA 94720; and [d]Department of Chemical Engineering, Carnegie Mellon University, Pittsburgh, PA 15213

Edited by Charles E. Kolb, Aerodyne Research, Inc., Billerica, MA, and accepted by Editorial Board Member A. R. Ravishankara May 17, 2017 (received for review December 20, 2016)

On-road gasoline vehicles are a major source of secondary organic aerosol (SOA) in urban areas. We investigated SOA formation by oxidizing dilute, ambient-level exhaust concentrations from a fleet of on-road gasoline vehicles in a smog chamber. We measured less SOA formation from newer vehicles meeting more stringent emissions standards. This suggests that the natural replacement of older vehicles with newer ones that meet more stringent emissions standards should reduce SOA levels in urban environments. However, SOA production depends on both precursor concentrations (emissions) and atmospheric chemistry (SOA yields). We found a strongly nonlinear relationship between SOA formation and the ratio of nonmethane organic gas to oxides of nitrogen (NO_x) (NMOG:NO_x), which affects the fate of peroxy radicals. For example, changing the NMOG:NO_x from 4 to 10 ppbC/ppbNO_x increased the SOA yield from dilute gasoline vehicle exhaust by a factor of 8. We investigated the implications of this relationship for the Los Angeles area. Although organic gas emissions from gasoline vehicles in Los Angeles are expected to fall by almost 80% over the next two decades, we predict no reduction in SOA production from these emissions due to the effects of rising NMOG:NO_x on SOA yields. This highlights the importance of integrated emission control policies for NO_x and organic gases.

air pollution | atmospheric particulate matter | gasoline vehicles | secondary organic aerosol | NO_x

Organic aerosol (OA) is a major component of atmospheric fine particles, which pose serious health risks and strongly influence Earth's climate. OA is comprised of primary and secondary organic aerosol (POA and SOA). SOA is formed in the atmosphere from the oxidation of organic vapors (SOA precursors); POA is directly emitted by sources. Even in urban areas, SOA concentrations often exceed POA levels (1). Tailpipe emissions from on-road gasoline vehicles are an important source of SOA in urban environments (2–4). For most vehicles, SOA formation exceeds the POA emissions after a few hours of atmospheric oxidation (5, 6). Therefore, controlling SOA precursor emissions is needed to reduce human exposure to fine particulate matter.

Over the past several decades, increasingly stringent regulations have led to dramatic reductions in gasoline vehicle nonmethane organic gas (NMOG) emissions in the United States and elsewhere. These regulations were mainly driven by the need to reduce ozone production, but they also reduced SOA formation because a portion of NMOG comprises SOA precursors (4). However, the effectiveness of these regulations at reducing fine particulate matter exposure is not known because of large gaps in our understanding of SOA formation (7, 8).

Smog chamber experiments using dilute exhaust have been conducted to quantify the SOA formation of gasoline vehicle exhaust (5, 9–11). Less SOA is formed from newer, lower-NMOG–emitting vehicles that meet more stringent emissions standards than from older, higher-emitting vehicles (5, 10, 11). However, exhaust from newer vehicles have higher effective SOA yields (SOA production per unit mass of reacted precursors) than exhaust from older vehicles (5, 10, 11). Gordon et al. (5) hypothesize that newer vehicles emit a more potent mix of SOA precursors than older vehicles, but this hypothesis has not been tested because of gaps in our knowledge of SOA formation and the complex and incompletely speciated NMOG emissions. If true, this may reduce the benefits of recently promulgated stricter emissions standards for gasoline vehicles (e.g., California LEV-III regulations).

We comprehensively characterized the emissions from 59 light-duty gasoline vehicles and performed smog chamber experiments with a subset of the fleet (25 vehicles) to investigate the effects of tightening vehicle emissions standards on SOA formation. All vehicles were recruited from the California in-use fleet; they span a wide range of model years (MY, 1988–2014), manufacturers, and emissions control technologies/standards. For discussion, we categorize these vehicles by emission certification standard: pre-LEV vehicles (Tier 0 and Tier 1; MY1988–2003), LEV vehicles (transitional low-emission vehicles and low-emission vehicles; MY1991–2012), ULEV vehicles (ultra–low-emission vehicles; MY2003–2013), and SULEV vehicles (super–ultra-low and partial–zero-emission vehicles; MY2012–2014) (*SI Appendix*). SULEV vehicles meet the most stringent emissions standard under the California LEV-II regulations.

California is phasing in even stricter LEV-III regulations for model years 2015–2025 (A comparable set of federal standards, Tier 3, is also being implemented over this time period). SULEV emissions are comparable to those from an average LEV-III

Significance

Secondary organic aerosol (SOA) is a major component of atmospheric fine particles, which pose serious health risks and influence Earth's climate. We combine laboratory measurements and computational modeling to investigate SOA formation from gasoline vehicle exhaust—an important source of air pollution in urban environments. We find a strong dependence of SOA formation from gasoline vehicle exhaust on oxides of nitrogen (NO_x) concentrations. Our results suggest that changing atmospheric NO_x levels over the next two decades will likely dramatically reduce the effectiveness of stricter new gasoline vehicle emissions standards to lower SOA concentrations in Los Angeles and other urban areas.

Author contributions: Y.Z. and A.L.R. designed research; Y.Z., R.S., G.S., A.A.P., T.D.G., G.T.D., A.H.G., and A.L.R. performed research; Y.Z., T.D.G., G.T.D., A.H.G., N.M.D., and A.L.R. analyzed data; N.M.D. contributed significant discussions and inputs; and Y.Z. and A.L.R. wrote the paper with input from all authors.

The authors declare no conflict of interest.

This article is a PNAS Direct Submission. C.E.K. is a guest editor invited by the Editorial Board.

[1]Present address: College of Engineering, University of Georgia, Athens, GA 30602.

[2]Present address: Handix Scientific, Boulder, CO 80301.

[3]To whom correspondence should be addressed. Email: alr@andrew.cmu.edu.

This article contains supporting information online at www.pnas.org/lookup/suppl/doi:10.1073/pnas.1620911114/-/DCSupplemental.

vehicle in model year 2025 (12). Therefore, our results provide insight into the potential effectiveness of the recently promulgated regulations to reduce SOA formation from on-road gasoline vehicles.

Our experiments follow the approach of Gordon et al. (5). We tested each vehicle on a chassis dynamometer using the cold-start Unified Cycle, which simulates southern California driving. We sampled the entire tailpipe emissions using a constant-volume sampler (CVS) from which dilute exhaust was collected for chemical analysis. For a subset (n = 25) of the vehicles, we transferred dilute exhaust from the CVS through a passivated, heated line into a 7 m^3 smog chamber equipped with black lights (model F40BL UVA, General Electric) to initiate photochemistry. The oxidation phase of the experiments typically lasted 3 h, which corresponded to 3–13 h of atmospheric processing at an OH concentration of 1.5 × 10^6 molecules cm^{-3}. We provide additional experimental details in *SI Appendix*.

Results and Discussion

In Fig. 1, we present NMOG emissions and SOA production data from the 25 vehicles tested in the smog chamber. Here "NMOG" refers to nonmethane organic gases measured by flame ionization detection (FID), which responds to both hydrocarbons and oxygenated compounds (13). The SOA production data have been corrected for wall losses (*SI Appendix*).

Fig. 1*A* shows that NMOG emissions decreased by 98% from the median pre-LEV to the median SULEV vehicle, underscoring the effectiveness of the tightening of emissions standards. We measured less SOA production from low-emitting vehicles (Fig. 1*B*). Therefore, tightening tailpipe emissions standards also reduces SOA formation from gasoline vehicle exhaust. However, the reductions in SOA production are less than the decrease in NMOG emissions. For example, ULEV vehicles have about a factor of 20 lower NMOG emissions compared with pre-LEV vehicles, but only a factor of 3 less SOA production. This raises concerns about the effectiveness of new emissions standards at reducing SOA in urban areas.

SULEV vehicles have the lowest SOA production, comparable to the average SOA production (~2 mg SOA/kg fuel) measured during dynamic blank experiments when the chamber was only filled with dilution air from the CVS (no exhaust) (*SI Appendix*). This complicates quantifying SOA production from SULEV vehicles because the dynamic blank likely overestimates background contamination (14). However, it is clear that SOA production from SULEV vehicles is very low. We did measure SOA formation from SULEV vehicles during parallel experiments conducted with an oxidation flow reactor that featured higher NMOG concentrations and higher oxidant exposures.

The trend in SOA production relative to NMOG emissions can be quantified in terms of an effective SOA yield, defined as the measured SOA mass divided by the mass of reacted SOA precursors (*SI Appendix*). As described below, only a subset of the NMOG emissions are SOA precursors. We calculated the mass of reacted SOA precursors in each experiment using the measured initial SOA precursor concentrations and OH exposure (*SI Appendix*). Presenting the data as SOA yields accounts for any differences in SOA production due to different OH exposures between experiments.

Fig. 1*C* shows the distribution of effective SOA mass yields by vehicle class. Exhaust from lower-NMOG–emitting vehicles has higher SOA yields, increasing from 0.05 ± 0.03 (avg ± SD) for pre-LEV to 0.30 ± 0.13 for LEV and 0.48 ± 0.18 for ULEV vehicles. Although the very low SOA production from SULEV vehicles makes any estimate of the SOA yield highly uncertain (Fig. 1*B*), the NMOG composition data discussed below suggest that SOA formation potential of SULEV exhaust is similar to LEV and ULEV vehicles. The trend in effective SOA yields by vehicle class is not due to differences in OA concentrations in the smog chamber (5) or biases due to the wall losses of condensable

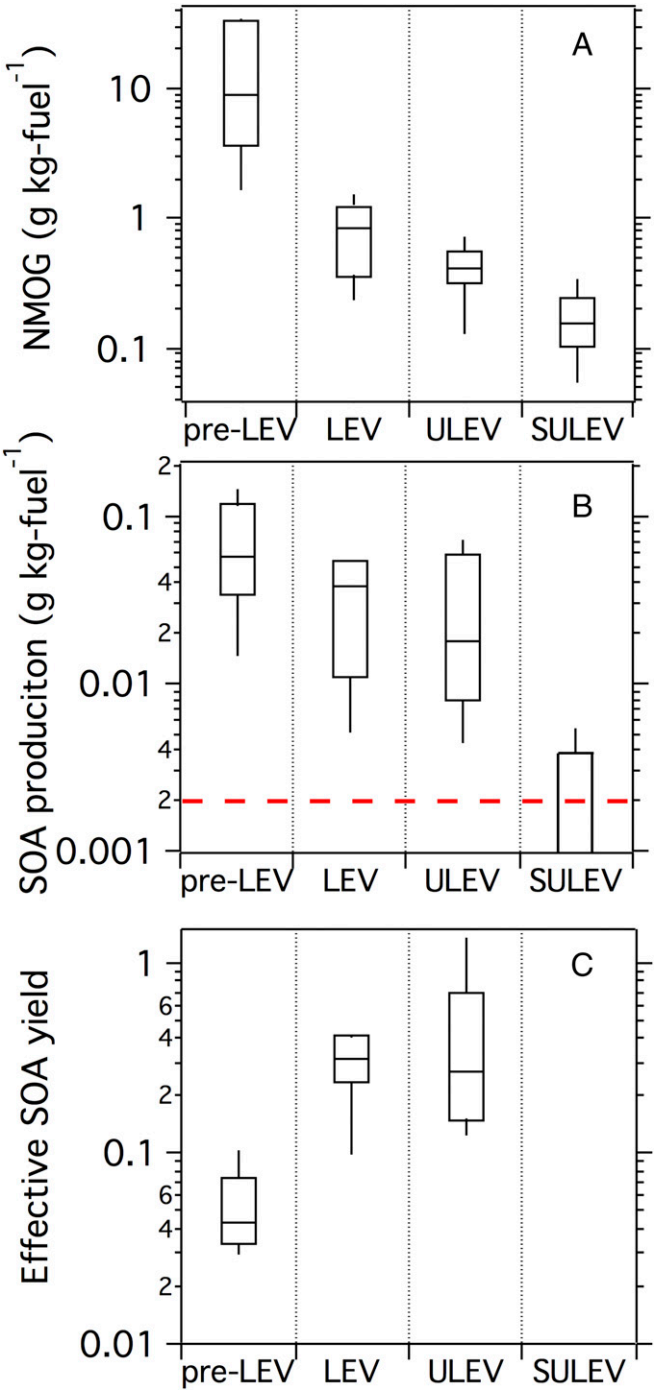

Fig. 1. Emissions and SOA production data from photooxidation experiments with dilute gasoline vehicle exhaust for different vehicle classes: (*A*) NMOG emissions, (*B*) end-of-experiment SOA production, and (*C*) effective SOA yields. The boxes represent the 75th and 25th percentiles of the data from individual vehicle tests with the centerline being the median. The whiskers are the 90th and 10th percentiles. The SOA production from SULEV was comparable to that measured during dynamic blank experiments, indicated by the dashed line in *B*. As discussed in the text, the SOA yields for SULEV vehicles were not estimated due to the large uncertainty in SOA production. This figure combines data from 14 newly tested vehicles (1 pre-LEV, 3 LEV, 3 ULEV, and 7 SULEV vehicles) with previously published data for 11 additional vehicles (3 pre-LEV, 3 LEV, and 5 ULEV vehicles) from Gordon et al. (5).

vapors (*SI Appendix*). For example, the median OA concentration in the smog chamber during the pre-LEV experiments was ~3 times higher than during ULEV experiments; this shifts gas-particle partitioning of semivolatile organics toward the condensed phase and increases SOA yields, which is opposite to the trend in the actual data.

To investigate the trend in SOA formation by vehicle class, we comprehensively characterized the NMOG emissions. We quantified almost 300 individual compounds and lumped components consisting of a group of compounds with similar volatility and molecular structure, including volatile organic compounds (VOCs), intermediate volatility organic compounds (IVOCs), and semivolatile organic compounds (SVOCs) (*SI Appendix*).

Fig. 2*A* presents the median NMOG composition for each vehicle class. Speciated VOC hydrocarbons (~200 species) are the largest component, contributing 66 ± 27% of the total NMOG mass across all tests. This includes important SOA precursors such as single-ring aromatics (19 ± 9% of NMOG emissions). Oxygenated VOCs with carbon number ≤ 6, including aldehydes, ketones, and alcohols, contribute 3.6 ± 2.7% of NMOG emissions (Fig. 2*A*). These species likely dominate the oxygenated organic emissions (15), but are unlikely to be SOA precursors in our experiments because of their low molecular weight and our use of nonacidic seed particles (16). Higher molecular weight hydrocarbons (IVOCs and SVOCs) contribute 5.3 ± 2.8% of the total NMOG. IVOCs and SVOCs have saturation concentrations (C^*) of 300 to 3×10^6 μg m^{-3} and 0.3–300 μg m^{-3}, respectively, corresponding approximately to C_{12}–C_{22} and C_{23}–C_{32} *n*-alkanes (6). We characterized IVOCs and SVOCs by analyzing sorbent and quartz filter samples using GC/mass spectrometry, which enabled quantification of 57 individual compounds and 32 lumped components (*SI Appendix*).

Despite our comprehensive analysis, 26 ± 13% of the NMOG mass measured by FID remains uncharacterized (which we refer to as "residual NMOG") (Fig. 2*A*). The most likely contributor to the residual NMOG is unidentified VOCs in the C^* range of C_2–C_{12} *n*-alkanes. Unlike our quantification of IVOCs and SVOCs, VOC analysis was only performed for a target list of compounds (*SI Appendix*), which almost certainly does not include all species in the VOC range (17). Larger (>C_6) oxygenated species also likely contribute some residual NMOG, but our data show that the majority (75 ± 8%) of measured oxygenated emissions are C_1 and C_2 species (formaldehyde and acetaldehyde). Furthermore, there is no relationship between emissions of oxygenated organics and the residual NMOG (*SI Appendix*, Fig. S1). Therefore, we believe the residual NMOG in our experiments is unlikely to contain significant additional SOA precursors.

Our comprehensive speciation analysis reveals that the NMOG composition is largely consistent across vehicle classes (Fig. 2 and *SI Appendix*, Fig. S2). The median NMOG composition for ULEV and SULEV vehicles is modestly different from the other classes with somewhat lower fractional aromatic and alkane emissions (and therefore higher residual NMOG), but these differences are not statistically significant and likely due to greater uncertainty associated with lower emission rates. This consistency also exists between individual vehicles (*SI Appendix*, Fig. S2), even though the absolute NMOG emission rates vary by almost two orders of magnitude across the test fleet.

The consistency in NMOG composition suggests that exhaust from different vehicles should have similar effective SOA yields. However, this contrasts sharply with the large measured variation in effective SOA yields. Fig. 2*B* compares the predicted effective SOA yields by vehicle class, using published high-NO_x (oxides of nitrogen) yield data for individual compounds (*SI Appendix*). Only a portion of quantified VOCs (e.g., single-ring aromatics and large alkanes) are known SOA precursors. All IVOCs and SVOCs are SOA precursors (*SI Appendix*). Although LEV, ULEV, and SULEV experiments had high ozone concentrations, unsaturated compounds are not expected to be an important source of SOA production in our study because 88 ± 11% of the alkenes were smaller than C_4 and there was no relationship between SOA yield and O_3 exposure (*SI Appendix*, Fig. S3). As discussed above, we assume that the residual NMOG does not contain significant additional SOA precursors.

Fig. 2*B* highlights the importance of IVOCs and SVOCs, which contribute only ~5% of the NMOG emissions but 45–76% of the predicted SOA. The predicted effective SOA yields estimated from the composition data increase for lower-NMOG–emitting vehicles because of the increasing importance of SVOCs. However, the predicted increase in SOA yields is much smaller than the observed increase. For example, the median predicted effective SOA yield only varies by a factor of 1.2 between pre-LEV and ULEV vehicles versus a factor of 6 for the measured data. Therefore, the measured differences in chemical composition between vehicle classes alone cannot explain the observed trend in effective SOA yields.

SOA yields also depend on radical chemistry, especially the effects of NO_x (specifically NO) on the fate of peroxy radicals (8, 18–21), similar to the well-known ozone EKMA relationship. Laboratory data indicate that NO_x effects depend strongly on

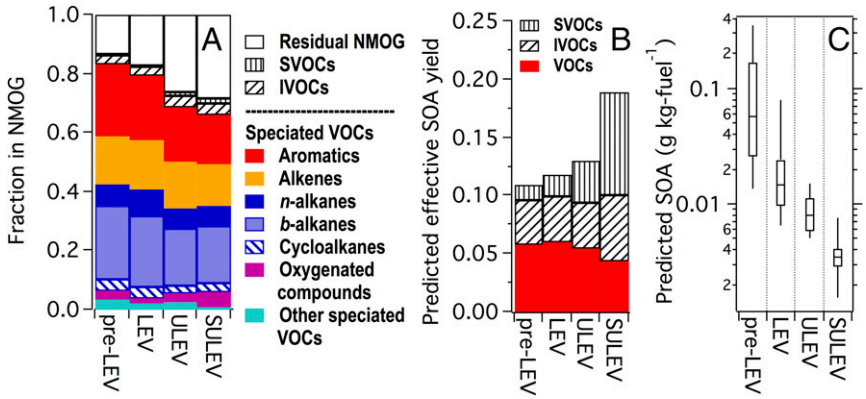

Fig. 2. NMOG composition and predicted SOA formation for different vehicle classes. (*A*) Median mass fractions of major NMOG components from all experiments by vehicle class. Speciated VOCs consisted of hydrocarbons with carbon number of 2–12 and oxygenated compounds with carbon number of ≤6. The majority of IVOCs and SVOCs were not speciated at a molecular level. (*B*) Median predicted effective SOA yields and (*C*) box-whisker plot of predicted SOA production. The predicted effective SOA yield and SOA production were calculated using the measured precursors, published high-NO_x yields data at an OA concentration of 10 μg/m^3, and an OH concentration of 1.5×10^6 molecules/cm^3 after 6-h photooxidation (*SI Appendix*). In *C*, the boxes represent the 75th and 25th percentiles with the centerline being the median. The whiskers are the 90th and 10th percentiles.

molecular structure of the SOA precursor. For example, aromatic compounds have much higher SOA yields at low-NO_x (high NMOG:NO_x) than high-NO_x conditions (low NMOG:NO_x) (18, 19, 22, 23), whereas SOA formation from large alkanes is less sensitive to NO_x (24). However, NO_x effects have only been investigated for a handful of compounds. Gasoline vehicle exhaust is a complex mixture of aromatics, alkanes, and other classes of compounds (6). Furthermore, the majority of IVOC and SVOC emissions from gasoline vehicles have not been resolved at the molecular level. Given this complexity, the NO_x effects on SOA formation from gasoline vehicle exhaust are uncertain.

Although the terms "high-NO_x" and "low-NO_x" are common, the fate of most organoperoxy radicals (RO_2) depends principally on NO concentrations. If substantial NO is present, then RO_2 + NO reactions dominate, creating "high-NO_x conditions"; at very low NO levels, RO_2 + HO_2 and RO_2 + RO_2 reactions will dominate, creating "low-NOx conditions". The major exception is peroxyacyl radicals, where peroxyacyl + NO_2 produces the peroxyacyl nitrates (PAN). However, the NO_x effects on SOA yields depend mostly on the NO concentrations in the chamber or the ambient atmosphere.

All of the experiments described here were conducted with high-NO_x concentrations, but there were large differences in NO levels. NO_x in vehicle exhaust is primarily NO; therefore the UV light portion of each experiment started with 41 ppbv or more of NO. Furthermore, photolysis of HONO produced NO. However, the NO reacted quickly with O_3 to form NO_2. During LEV, ULEV, and SULEV experiments, NO levels fell below the detection limit of our instrument (a few ppbv) within minutes of turning on the UV lights, which led to a rapid increase in ozone concentrations (*SI Appendix*, Fig. S4). Therefore, essentially all of the SOA formation during these experiments occurred at very low NO levels (*SI Appendix*, Fig. S5). In contrast, NO levels were high throughout the pre-LEV experiments (the vehicles with the highest NO emissions), which resulted in low ozone concentrations. Therefore, the SOA formation in pre-LEV experiments occurred at high NO levels (*SI Appendix*, Fig. S5). Therefore, the LEV, ULEV, and SULEV experiments were likely conducted in a different NO_x regime than the pre-LEV experiments.

The different NO_x regimes can be indicated by the NMOG:NO_x (which is analogous to the ratio of volatile organic compounds to NO_x or VOC:NO_x used in policy making) (25). We added propene to the chamber to adjust the initial NMOG:NO_x (5), but interferences associated with HONO and the chemiluminescence NO_x analyzer caused the experiments to span a wide range of initial NMOG:NO_x (*SI Appendix*). These interferences only affect NO_2 measurements. Because NO_2 only contributed 6.6 ± 5.3% of the vehicular NO_x emissions on a molar basis, we can robustly estimate the initial NMOG:NO_x using the measured NO. Although we added similar amounts of HONO and propene in each experiment (*SI Appendix*), the effect of the HONO interference was larger for low-emitting vehicles because of lower exhaust NO_x levels in the chamber. Therefore, the net effect of the propene addition created a systematic trend in the initial NMOG:NO_x by vehicle class ranging from 4.2 ± 1.0, 8.4 ± 4.4, 10.3 ± 4.3, and 17.8 ± 20.3 ppb C/ppb NO_x for pre-LEV, LEV, ULEV, and SULEV experiments, respectively.

Our experiments allow examination of the effects of NO on SOA formation from gasoline vehicle exhaust, a highly complex mixture of organics. However, because VOC:NO_x is the common descriptor in policy making, we present our results in terms of NMOG:NO_x. Fig. 3*A* presents the effective SOA yield as a function of the initial NMOG:NO_x. The yield increases dramatically with increasing NMOG:NO_x. To quantify this increase, we binned the data and fitted a natural exponential to the average value in each NMOG:NO_x bin (red symbols). This is an empirical relationship based on the initial NMOG:NO_x of these experiments. The effective SOA yield increased from 0.06 to 0.46 as the NMOG:NO_x increased from 4 to 10, after which the yield was approximately constant. This increase in SOA yield is important because the NMOG:NO_x in many urban areas is evolving across this range as more controls are implemented on NO_x emissions (Fig. 3 *A* and *B*).

The measured increase in the effective SOA yield of gasoline vehicle exhaust is at the high end of the range observed for the handful of individual compounds whose changes in yield with NMOG:NO_x have been previously studied (18, 19). Of these compounds, the largest increases in SOA production with

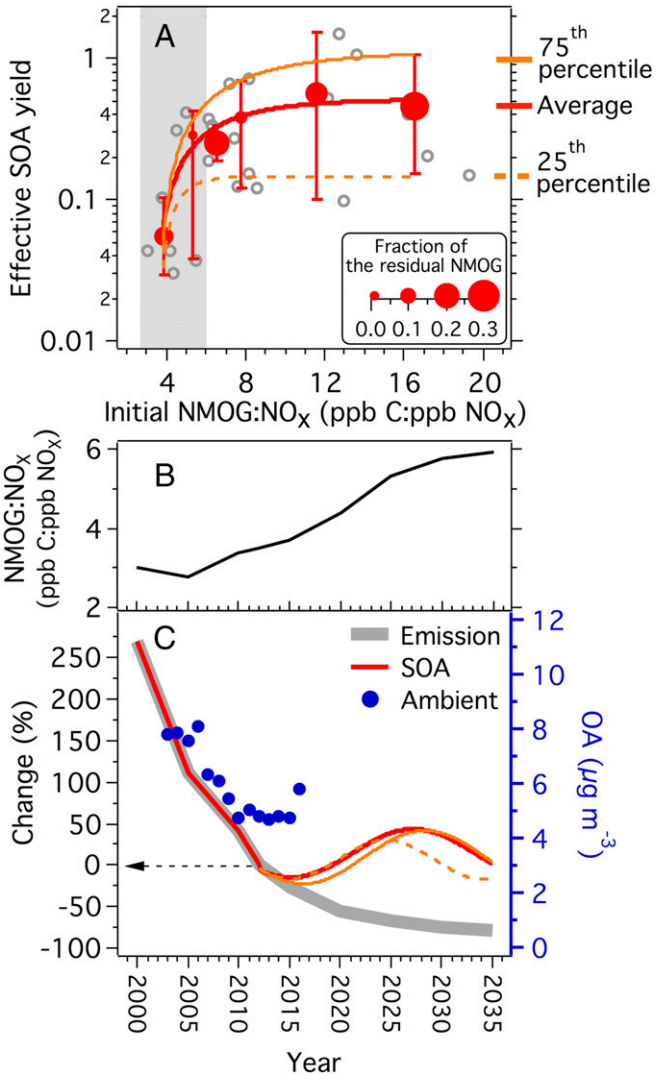

Fig. 3. Effect of NMOG:NO_x on SOA production in the Los Angeles Area. (*A*) Empirical relationship between effective SOA yield (defined as the ratio of SOA mass to the reacted mass of SOA precursors) as a function of the initial ratio of NMOG to NO_x (NMOG:NO_x) during photooxidation experiments with pre-LEV, LEV, and ULEV vehicles. The red points are averages, and the vertical red bar indicates the maximum and minimum of effective SOA yields within each NMOG:NO_x bin. The red line shows the fit of the average data; orange dashed and solid lines show fits of the 25th and 75th percentiles of the effective SOA yields in each NMOG:NO_x bin. (*B*) Predicted NMOG:NO_x in the South Coast Air Basin (SoCAB) over the period from 2000 to 2035 (also shown as the gray region in *A*). (*C*) Predicted changes in on-road gasoline vehicle NMOG emissions (gray curve) and SOA production (red curve) from these emissions in the SoCAB normalized to the base year of 2012. The prediction of SOA production has accounted for changes in NMOG:NOx. The blue symbols in *C* are the measured annual average OA concentrations, calculated by multiplying the PM2.5 organic carbon measured in Los Angeles by the Chemical Speciation Network (*SI Appendix*) by a factor of 1.7 (4). The arrow marks the value of "zero" on the *y* axis, which corresponds to the base year of 2012.

NMOG:NO_x have been reported for single-ring aromatics (19). For gasoline vehicle exhaust, the majority of SOA production from VOCs is from single-ring aromatics. Aromatics (higher molecular weight single-ring and polyaromatics) likely also dominate SOA production from IVOCs (6).

As a final step in our analysis, we quantitatively compared the measurements to predictions of an SOA model (*SI Appendix*). Briefly, model inputs included measured SOA precursor (VOCs, IVOCs, and SVOCs) concentrations and OH exposures. We used yield data from the literature that account for both measured OA concentrations inside the chamber (gas-particle partitioning) and NO_x effects (low versus high NMOG:NO_x) (*SI Appendix*).

We can explain the measured SOA formation of gasoline vehicle exhaust if we account for all measured SOA precursors and NO_x effects. In Fig. 4 we present model–measurement comparisons for high- and low-NO_x conditions. Except for the pre-LEV experiments, the high-NO_x predictions substantially underestimate measured SOA production with a median model–measurement ratio of 0.44. We conducted the pre-LEV experiments at high-NO_x conditions. The low-NO_x predictions largely close the SOA mass balance for LEV and ULEV experiments conducted at high initial NMOG:NO_x with the median model–measurement ratio of 0.97. This supports the conclusion that the trend in effective SOA yields among vehicle classes shown in Fig. 1*C* is primarily due to the effects of NO_x (i.e., different experimental conditions) and not differences in exhaust composition.

Our SOA predictions are uncertain due to uncertainties in both published SOA yield data and wall losses of low-volatility organic vapors. For example, published SOA yields of *m*-xylene under high-NO_x conditions at the OA concentration of 10 $\mu g/m^3$ vary by a factor of ~2.5 (19, 26, 27). We used parameterizations at the high end of the published range. In addition, we measured SOA precursors in the CVS and assumed that they were transferred to the chamber with 100% efficiency (neglecting possible losses of low-volatility organic vapors). This approach provides an upper bound on the SOA precursor concentration inside the chamber, which, in turn, provides an upper bound on the estimated SOA production. These two factors (high yields and assuming negligible wall losses) likely explain the model overprediction of the pre-LEV data.

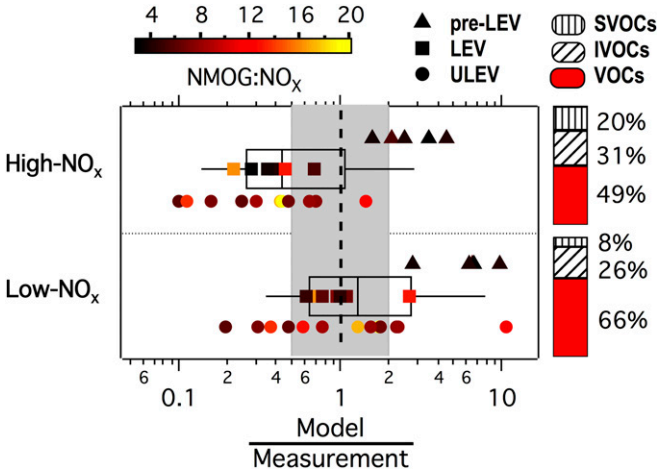

Fig. 4. Ratio of model-predicted to measured SOA for high- and low-NO_x conditions. The boxes represent the 75th and 25th percentiles with the centerline being the median. The whiskers are the 90th and 10th percentiles. The symbols show the model-to-measurement ratios for individual experiments, color-coded by their initial NMOG:NO_x. The gray-shaded area indicates the range of the model-to-measurement SOA ratio from 0.5 to 2 with the vertical dash line being the ratio of 1. The bars on the right present the average contribution of each class of SOA precursors to the total predicted SOA production. SULEV data are not included because SOA formation was comparable to the dynamic blank.

These uncertainties do not depend on vehicle class and therefore should not alter the observed trend in SOA production by vehicle class. In addition, our assumption of negligible wall losses for low-volatility vapors barely alters the trend of observed effective SOA yields. For example, excluding SVOCs from the model reduces predicted SOA production by 20% (Fig. 4, the high-NO_x case), but only increases the effective SOA yield by 4%, on average.

Fig. 4 indicates that IVOCs and SVOCs contribute 34–51% of the predicted SOA in our chamber experiments, confirming the hypothesis of Jathar et al. (3) that unspeciated NMOG (the sum of IVOCs, SVOCs, and residual NMOG in the present study) is an important source of SOA precursors. We have now quantified IVOCs and SVOCs, and although they are only a small fraction of the unspeciated NMOG of Jathar et al. (3), they comprise the vast majority of the additional precursors. The effective SOA yields presented in Fig. 3*A* show no positive correlation with the fraction of the residual NMOG, supporting the conclusion that the residual (uncharacterized) NMOG are not significant SOA precursors.

Our experiments demonstrate that increasingly stringent NMOG emissions standards reduce SOA precursor emissions (Fig. 1 and *SI Appendix*, Fig. S6). For example, emissions of major classes of SOA precursors (single-ring aromatics and IVOCs) mirror the reductions in NMOG across vehicle classes (*SI Appendix*, Fig. S6). This should reduce SOA production from gasoline vehicle exhaust provided that the atmospheric NMOG:NO_x remains in the high-NO_x regime where RO_2 + NO dominates (Fig. 2*C*). The exception is SVOC emissions, for which tightening NMOG emissions standards has been relatively less effective at controlling compared with other SOA precursor classes (e.g., Fig. 2). This may be due to lubricating oil and not fuel being the major source of SVOC emissions (28, 29) (*SI Appendix*).

However, the strong dependence of the SOA yield on NMOG:NO_x can dramatically influence the effectiveness of gasoline vehicle emission controls (and NMOG controls in general) on SOA formation. Fig. 3*C* shows that the California Air Resources Board (CARB) predicts an 80% reduction in NMOG emissions from on-road gasoline vehicles over the next two decades (with the base year of 2012) in the South Coast Air Basin (SoCAB) due to fleet turnover and widespread deployment of vehicles meeting SULEV standards (12, 30). If the NMOG:NO_x remained constant, this would lead to a dramatic reduction in SOA formation. However, over this period, CARB predicts that the average atmospheric NMOG:NO_x in the SoCAB will increase from 3.5 to 6.0 due to large reductions in NO_x emissions necessary for ozone and inorganic particulate matter controls (Fig. 3*B* and *SI Appendix*, Fig. S7) (30). Similar changes in NMOG:NO_x are occurring in other parts of the United States (31). NMOG:NO_x also varies by time of day and day of the week—e.g., NMOG:NO_x is higher on weekends when there is less diesel truck traffic (32, 33).

In Fig. 3*C* we show the effect of changing NMOG:NO_x on SOA production from gasoline vehicles in the SoCAB (Los Angeles and vicinity), including historical data from 2003 and extending to 2035. Our calculations combine the CARB-predicted NMOG:NO_x (Fig. 3*B*) and CARB on-road gasoline vehicle NMOG emission inventory (*SI Appendix*, Fig. S7) with our effective SOA yield data (Fig. 3*A*). We assume a constant effective SOA yield of 0.06 for NMOG:$NO_x \leq 4.1$, which corresponds to the conditions in Los Angeles before 2012 (2).

Fig. 3*C* suggests that historical controls have been highly effective at reducing SOA levels in the Los Angeles area. Before 2012, atmospheric OA levels declined at 8% per year, mirroring the reductions in gasoline vehicle NMOG emissions. However, our results indicate that future reductions in these emissions may not lead to lower SOA levels due to increasing SOA yields caused by changing NMOG:NO_x. In fact, our predictions suggest

that for the majority of the 2020–2035 period the SOA production from on-road gasoline vehicles will be greater than in 2012. The ambient OA data have been essentially constant since 2012, suggesting that this leveling off may have already begun.

Therefore, despite widespread adoption of SULEV-compliant vehicles over the next two decades, our data suggest that there will be little reduction in SOA from gasoline vehicle emissions. In contrast, emissions reductions before 2012 occurred under high-NO_x conditions (2) (Fig. 3*C*) and thus were highly effective at reducing SOA formation. Although there is variability in the measured yields, predictions based on the 25th and 75th percentiles of the yield data suggest that this conclusion is robust (Fig. 3*C*).

Reducing NO_x emissions is important for ozone and inorganic particulate matter controls (34), but Fig. 3*C* suggests that there will be a large unintended consequence of this strategy on SOA production (and therefore urban particulate matter levels). This is an important tradeoff because most of the economic benefits attributed to reductions in air pollution are associated with reductions in particulate matter concentrations (35). Reducing NO_x will reduce nitrate aerosol, but these reductions will likely be offset to some extent by higher [and potentially more toxic (36)] SOA levels. It is likely the same effect will occur in many urban areas. In addition, although our analysis only considered on-road gasoline vehicle exhaust (an important source of SOA precursors in urban environments), SOA production from emissions from other sources also likely depends on NMOG:NO_x. Our findings highlight the importance of integrated emission control policies for NO_x and NMOGs to maximize the benefits of recently promulgated vehicle emissions standards.

Materials and Methods

We characterized the tailpipe emissions from on-road gasoline vehicles and their SOA production during dynamometer testing at the California Air Resources Board's (CARB) Haagen–Smit Laboratory. We sampled the entire exhaust from each vehicle using a constant-volume sampler (CVS) nominally following the Code of Federal Regulations Title 40, Chapter 1, Subchapter C, Part 86. We converted pollutant concentrations measured in the CVS and smog chamber to a fuel basis using measured CO_2 and CO concentrations and a fuel-carbon mass-balance approach. We quantified SOA precursor emissions through comprehensive analysis of samples collected from the CVS using Tedlar bags, 1,4-dinitrophenylhydrazine (DNPH) impregnated cartridges, Tenax adsorbent tubes, and quartz filters. We photooxidized dilute emissions from 25 vehicles in a 7 m^3 smog chamber to quantify SOA production. We corrected the SOA production data for vapor and particle wall losses. We predicted the SOA production using the measured SOA precursor emissions, OH concentrations inferred from the measured decay of *d*-butanol, and the approach of Zhao et al. (6). Please see *SI Appendix* for further details of materials and methods.

ACKNOWLEDGMENTS. The authors would like to thank the excellent and dedicated personnel at the California Air Resources Board, especially at the Haagen–Smit Laboratory. Financial support was provided by the California Air Resources Board (Contract #12-318) and US Environmental Protection Agency (Assistance Agreement RD83587301). The California Air Resources Board also provided substantial in-kind support for vehicle procurement, testing, and emissions characterization. The views, opinions, and/or findings contained in this paper are those of the authors and should not be construed as an official position of the funding agencies.

1. Jimenez JL, et al. (2009) Evolution of organic aerosols in the atmosphere. *Science* 326: 1525–1529.
2. Hayes PL, et al. (2013) Organic aerosol composition and sources in Pasadena, California, during the 2010 CalNex campaign. *J Geophys Res* 118:9233–9257.
3. Jathar SH, et al. (2014) Unspeciated organic emissions from combustion sources and their influence on the secondary organic aerosol budget in the United States. *Proc Natl Acad Sci USA* 111:10473–10478.
4. McDonald BC, Goldstein AH, Harley RA (2015) Long-term trends in California mobile source emissions and ambient concentrations of black carbon and organic aerosol. *Environ Sci Technol* 49:5178–5188.
5. Gordon TD, et al. (2014) Secondary organic aerosol formation exceeds primary particulate matter emissions for light-duty gasoline vehicles. *Atmos Chem Phys* 14:4661–4678.
6. Zhao Y, et al. (2016) Intermediate volatility organic compound emissions from on-road gasoline vehicles and small off-road gasoline engines. *Environ Sci Technol* 50:4554–4563.
7. Hallquist M, et al. (2009) The formation, properties and impact of secondary organic aerosol: Current and emerging issues. *Atmos Chem Phys* 9:5155–5236.
8. Kroll JH, Seinfeld JH (2008) Chemistry of secondary organic aerosol: Formation and evolution of low-volatility organics in the atmosphere. *Atmos Environ* 42:3593–3624.
9. Liu T, et al. (2015) Secondary organic aerosol formation from photochemical aging of light-duty gasoline vehicle exhausts in a smog chamber. *Atmos Chem Phys* 15:9049–9062.
10. Nordin EZ, et al. (2013) Secondary organic aerosol formation from idling gasoline passenger vehicle emissions investigated in a smog chamber. *Atmos Chem Phys* 13: 6101–6116.
11. Platt SM, et al. (2013) Secondary organic aerosol formation from gasoline vehicle emissions in a new mobile environmental reaction chamber. *Atmos Chem Phys* 13: 9141–9158.
12. CARB (2012) California Air Resources Board, "LEV III" Amendments to the California Greenhouse Gas and Criteria Pollution Exhaust and Evaporative Emission Standards and Test Procedures and to the On-Board Diagnostic System Requirements for Passenger Cars, Light-Duty Trucks, and Medium-Duty Vehicles, and to the Evaporative Emission Requirements for Heavy-Duty Vehicles. Available at www.arb.ca.gov/regact/2012/leviiighg2012/levfrorev.pdf. Accessed October 8, 2016.
13. Scanlon JT, Willis JT (1985) Calculation of flame ionization detector relative response factors using the effective carbon number concept. *J Chromatogr Sci* 23:333–340.
14. May AA, et al. (2014) Gas- and particle-phase primary emissions from in-use, on-road gasoline and diesel vehicles. *Atmos Environ* 88:247–260.
15. Schauer JJ, Kleeman MJ, Cass GR, Simoneit BRT (2002) Measurement of emissions from air pollution sources. 5. C1-C32 organic compounds from gasoline-powered motor vehicles. *Environ Sci Technol* 36:1169–1180.
16. Kroll JH, et al. (2005) Chamber studies of secondary organic aerosol growth by reactive uptake of simple carbonyl compounds. *J Geophys Res* 110:D23207.
17. Goldstein AH, Galbally IE (2007) Known and unknown organic constituents in the Earth' s atmosphere. *Environ Sci Technol* 41:1514–1521.
18. Chan AWH, et al. (2009) Secondary organic aerosol formation from photooxidation of naphthalene and alkylnaphthalenes: Implications for oxidation of intermediate volatility organic compounds (IVOCs). *Atmos Chem Phys* 9:3049–3060.
19. Ng NL, et al. (2007) Secondary organic aerosol formation from m-xylene, toluene, and benzene. *Atmos Chem Phys* 7:3909–3922.
20. Presto AA, Hartz KEH, Donahue NM (2005) Secondary organic aerosol production from terpene ozonolysis. 2. Effect of NOx concentration. *Environ Sci Technol* 39: 7046–7054.
21. Zhang J, Huff Hartz KE, Pandis SN, Donahue NM (2006) Secondary organic aerosol formation from limonene ozonolysis: Homogeneous and heterogeneous influences as a function of NO(x). *J Phys Chem A* 110:11053–11063.
22. Hildebrandt L, Donahue NM, Pandis SN (2009) High formation of secondary organic aerosol from the photo-oxidation of toluene. *Atmos Chem Phys* 9:2973–2986.
23. Li LJ, Tang P, Cocker DR (2015) Instantaneous nitric oxide effect on secondary organic aerosol formation from m-xylene photooxidation. *Atmos Environ* 119:144–155.
24. Cappa CD, et al. (2013) Application of the Statistical Oxidation Model (SOM) to Secondary Organic Aerosol formation from photooxidation of C-12 alkanes. *Atmos Chem Phys* 13:1591–1606.
25. Seinfeld JH, Pandis SN (2006) *Atmospheric Chemistry and Physics: From Air Pollution to Climate Change* (John Wiley & Sons, Hoboken, NJ).
26. Odum JR, et al. (1996) Gas/particle partitioning and secondary organic aerosol yields. *Environ Sci Technol* 30:2580–2585.
27. Song C, Na K, Cocker DR, 3rd (2005) Impact of the hydrocarbon to NOx ratio on secondary organic aerosol formation. *Environ Sci Technol* 39:3143–3149.
28. Worton DR, et al. (2014) Lubricating oil dominates primary organic aerosol emissions from motor vehicles. *Environ Sci Technol* 48:3698–3706.
29. May AA, et al. (2013) Gas-particle partitioning of primary organic aerosol emissions: (1) Gasoline vehicle exhaust. *Atmos Environ* 77:128–139.
30. CARB (2013) California Air Resources Board. CEPAM: 2013 Almanac - Standard Emissions Tool. Emission Projections for ROG and NOx in South Coast Air Basin, California during 2012-2035. Available at www.arb.ca.gov/app/emsinv/fcemssumcat2013.php. Accessed May 15, 2016.
31. Russell AR, Valin LC, Cohen RC (2012) Trends in OMI NO2 observations over the United States: Effects of emission control technology and the economic recession. *Atmos Chem Phys* 12:12197–12209.
32. Fujita EM, Campbell DE, Stockwell WR, Lawson DR (2013) Past and future ozone trends in California's South Coast Air Basin: Reconciliation of ambient measurements with past and projected emission inventories. *J Air Waste Manag Assoc* 63:54–69.
33. Marr LC, Harley RA (2002) Modeling the effect of weekday-weekend differences in motor vehicle emissions on photochemical air pollution in central California. *Environ Sci Technol* 36:4099–4106.
34. South Coast Air Quality Management Distict (2013) Final 2012 Air Quality Management Plan. Available at www.aqmd.gov/home/library/clean-air-plans/air-quality-mgt-plan/final-2012-air-quality-management-plan (South Coast Air Quality Management District). Accessed June 30, 2016.
35. US Environmental Protection Agency (2011) Benefits and Costs of the Clean Air Act 1990-2020, the Second Prospective Study. Available at www.epa.gov/clean-air-act-overview/benefits-and-costs-clean-air-act-1990-2020-second-prospective-study. Accessed September 30, 2016.
36. Künzi L, et al. (2015) Toxicity of aged gasoline exhaust particles to normal and diseased airway epithelia. *Sci Rep* 5:11801.